Epilepsy Research 171 (2021) 106569

Contents lists available at ScienceDirect

Epilepsy Research

journal homepage: www.elsevier.com/locate/epilepsyres

# Functional connectivity disturbances of ascending reticular activating system and posterior thalamus in juvenile myoclonic epilepsy in relation with photosensitivity: A resting-state fMRI study

Emel Ur Özçelik [a,b,*], Elif Kurt [c], Nermin Görkem Şirin [a], Kardelen Eryürek [c,d], Çiğdem Ulaşoglu Yıldız [d], Emre Harı [c,d], Ulaş Ay [c,d], Nerses Bebek [a], Tamer Demiralp [d,e], Betül Baykan [a]

[a] Departments of Neurology and Clinical Neurophysiology, Istanbul University, Istanbul Faculty of Medicine, Millet Cad, 34093, Istanbul, Turkey
[b] Department of Neurology, Istanbul Bakirkoy Prof. Dr. Mazhar Osman Research and Training Hospital for Psychiatry, Neurology, Neurosurgery, University of Health Sciences, Zuhuratbaba Mahallesi, Dr. Tevfik Sağlam Cad. 25/2, 34147, Bakırkoy, Istanbul, Turkey
[c] Department of Neuroscience, Aziz Sancar Institute of Experimental Medicine, Istanbul University, Millet Cad, 34093, Çapa, Istanbul, Turkey
[d] Hulusi Behçet Life Sciences Research Laboratory, Neuroimaging Unit, Istanbul University, Millet Cad, 34093, Capa, Istanbul, Turkey
[e] Department of Physiology, Istanbul University, Istanbul Faculty of Medicine, Millet Cad, 34093, Capa, Istanbul, Turkey

ARTICLE INFO

*Keywords:*
Juvenile myoclonic epilepsy
Ascending reticular activating system
rResting- state fMRI
Photosensitivity
Posterior thalamus
Locus coeruleus

ABSTRACT

*Objective:* Juvenile myoclonic epilepsy (JME) is typified by the occurrence of myoclonic seizures after awakening, though another common trait is myoclonic seizures triggered by photic stimulation. We aimed to investigate the functional connectivity (FC) of nuclei in the ascending reticular activating system (ARAS), thalamus and visual cortex in JME with and without photosensitivity.

*Methods:* We examined 29 patients with JME (16 photosensitive (PS), 13 non- photosensitive-(NPS)) and 28 healthy controls (HCs) using resting-state functional magnetic resonance imaging (rs-fMRI). Seed-to-voxel FC analyses were performed using 25 seeds, including the thalamus, visual cortex, and ARAS nuclei.

*Results:* Mesencephalic reticular formation seed revealed significant hyperconnectivity between the bilateral paracingulate gyrus and anterior cingulate cortex in JME group, and in both JME-PS and JME-NPS subgroups compared to HCs ($p_{FWE\text{-}corr} < 0.001$; $p_{FWE\text{-}corr} < 0.001$; $p_{FWE\text{-}corr} = 0.002$, respectively). Locus coeruleus seed displayed significant hyperconnectivity with the bilateral lingual gyri, intracalcarine cortices, occipital poles and left occipital fusiform gyrus in JME-PS group compared to HCs ($p_{FWE\text{-}corr} < 0.001$). Additionally, locus coeruleus seed showed significant hyperconnectivity in JME-PS group compared to JME-NPS group with a cluster corresponding to the bilateral lingual gyri and right intracalcarine cortex ($p_{FWE\text{-}corr} < 0.001$). Lastly, the right posterior nuclei of thalamus revealed significant hyperconnectivity with the right superior lateral occipital cortex in JME-PS group compared to HCs ($p_{FWE\text{-}corr} < 0.002$).

*Conclusions:* In JME, altered functional connectivity of the arousal networks might contribute to the understanding of myoclonia after awakening, whereas increased connectivity of posterior thalamus might explain photosensitivity.

*Abbreviations:* ART, Artifact Detection Tools; EPI, Echo planar images; FCs, Functional connectivities; FD, Frame-wise displacement; FOV, Field of view; FWE, Family-wise error; GS, Global signal; LGN, Lateral geniculate nucleus; MNI, Normalized to the Montreal Neurological Institute; MRF, Mesencephalic reticular formation; NPS, Non-photosensitive; PS, Photosensitive; ROI, Regions of interest; SMA, Supplementary motor area; SPM 12, Statistical Parametric Mapping; TE, Echo time; TR, Repetition time; WM, White matter.

* Corresponding author at: Departments of Neurology and Clinical Neurophysiology, Istanbul University, Istanbul Faculty of Medicine, Millet Cad, 34093, Istanbul, Turkey.

*E-mail addresses:* emeluscas@gmail.com (E. Ur Özçelik), elifkurt@istanbul.edu.tr (E. Kurt), gorkemsirin@yahoo.com.tr (N.G. Şirin), eryurekkardelen@gmail.com (K. Eryürek), cigdemulasoglu@gmail.com (Ç. Ulaşoglu Yıldız), emrehr@hotmail.com (E. Harı), psk.ulasay@gmail.com (U. Ay), nersesb@yahoo.com (N. Bebek), demiralp.tamer@gmail.com (T. Demiralp), baykanb@istanbul.edu.tr (B. Baykan).

https://doi.org/10.1016/j.eplepsyres.2021.106569
Received 6 September 2020; Received in revised form 29 December 2020; Accepted 1 February 2021
Available online 3 February 2021
0920-1211/© 2021 Elsevier B.V. All rights reserved.

## 1. Introduction

Juvenile myoclonic epilepsy (JME) is a common genetic generalized epilepsy (GGE) and the typical myoclonic jerks after awakening in adolescence are the hallmark of this syndrome, essential for its diagnosis. Triggering seizures with flickering light and a photoparoxysmal response during electroencephalography (EEG) are also frequently observed in JME (Baykan and Wolf, 2017). Having seizures triggered by a sleep-wake transition and seizures triggered by visual stimuli suggest distinguishable neuro-anatomic substrates of epileptogenicity in JME. Historical studies in animals and humans have found that epileptogenicity can arise from cortical and subcortical structures (Gloor, 1968).

In recent years, epileptogenesis has been studied using resting-state functional magnetic resonance imaging (rs-fMRI) (Hamandi et al., 2006). Although many different results have been obtained from fMRI studies, GGE has been associated with dysfunction in several neural networks, especially in the prefrontal cortex and thalamus (Aghakhani et al., 2004; Holmes et al., 2010; Vollmar et al., 2011; Vaudano et al., 2009). A recent diffusion tensor imaging (DTI) study provided structural evidence that the midbrain and thalamus are likely to play a key role in human epilepsy (Xie et al., 2017).

Some animal models had already pointed out the role of the upper brainstem in generalized spike-wave discharges. A feline model of generalized epilepsy supported a leading role of cortical neurons in initiating and maintaining generalized spike-wave discharges that are temporally regulated by corticothalamocortical and reticulothalamic circuits (Gloor, 1968; Pellegrini et al., 1985).

The upper brainstem mesencephalic reticular formation (MRF) has also been shown to have a critical role in the initiation, maintenance, and control of generalized seizures in animal studies (Hashizume et al., 2000). The MRF is part of the ascending reticular activating system (ARAS) that regulates general arousal states and consists of nuclei dispersed within the brainstem reticular formation (Paus, 2000; Zeman, 2001; Jang and Kwon, 2015; Wijdicks, 2019). The ARAS plays an important role in maintaining or transitioning states of sleep, wakefulness, awareness, and consciousness (Edlow et al., 2012; Yeo et al., 2013). However, ARAS connectivity has not been studied much in epilepsy. Recent studies have demonstrated altered functional connectivity (FC) of ARAS in temporal lobe epilepsy (TLE) (González et al., 2019; Englot et al., 2018; Li et al., 2020). One DTI study demonsrated increased fractional anisotropy values in ARAS and thalamus in photosensitive JME patients (von Podewils et al., 2015).

JME has a close relationship to the sleep-wake cycle, especially during the transitional phase from sleep to wakefulness, with most patients showing myoclonia and occasional generalized tonic-clonic seizures upon awakening. The cortical excitability measured by transcranial magnetic stimulation increases early in the morning in JME, but not in subjects with focal epilepsy or controls without epilepsy (Badawy et al., 2009). This may explain the increased seizure susceptibility in this syndrome after awakening. However, the anatomical correlates of these changes have remained obscure; thus it is tempting to speculate that the ARAS may be the missing anatomical-physiological link in JME with typical seizures after awakening.

Since photosensitivity is a common reflex feature and might shed light on the pathogenesis of seizures in JME, it has attracted the attention of researchers. In several fMRI studies of JME patients with photoparoxysmal responses, it has been demonstrated that excessive neural activity in the visual cortex due to photic stimulation and connectivity abnormalities of visual areas with motor-premotor and subcortical regions causes the development of frontocentral discharges and seizures in these patients (Bartolini et al., 2014; Vollmar et al., 2012; Moeller et al., 2009).The role of the occipital cortex and posterior thalamus in the pathogenesis of JME has also been supported by different neurophysiological and neuroimaging studies (Zhong et al., 2018; Strigaro et al., 2015b; Brigo et al., 2013).

There is a limited number of fMRI studies demonstrating the resting status of neural networks, in which JME patients with and without photosensitivity are divided into subgroups. Also, previous fMRI studies conducted with photosensitive patients are mainly task-based, the evaluation of the resting status of the visual network between thalamic critical structures and cortical/subcortical areas are lacking (Moeller et al., 2009; Vollmar et al., 2012; Vaudano et al., 2017; Jiang et al., 2016; Hill et al., 1999). Moreover, despite the role of the ARAS in awakening and consciousness, an rs-fMRI study of the ARAS in JME has not yet been published.

We have mainly two working hypotheses for this study. First, given that seizures are very typical after awakening in JME, functional connectivities (FCs) of the ARAS nuclei should be different from healthy controls (HCs). Furthermore, since the daylight after awakening might have an effect on the seizures, there should also be differences in the FCs of visual neural networks and arousal networks between JME and the HCs. Second, since photic stimulation triggers myoclonia in only some patients with JME, there should be differences in the resting status FCs of these primary visual networks between the photosensitive JME (JME-PS) and non-photosensitive JME (JME-NPS) subgroups.

Therefore, we analyzed the FCs of relevant cortical and subcortical structures by rs-fMRI, taking the presence of photosensitivity as an endophenotype in JME.

## 2. Methods

### 2.1. Subjects

Thirty-one patients diagnosed with JME (sixteen JME-PS and fifteen JME-NPS) were recruited from the outpatient clinics of two epilepsy centers. Patients were included if they i) had a definite diagnosis of JME according to ILAE 2017 criteria (Scheffer et al., 2017), based on the clinical history, seizure types, neurologic examination and EEG features; ii) had seizures triggered by lack of sleep and/or light stimuli iii) were between the ages of 16–65 years with a minimum follow-up duration of one year; iv) do not have major psychiatric and any other neurologic diseases; v) do not have any contraindication for magnetic resonance imaging (MRI) or pregnancy. The timing of MRI recordings was organized to maintain seizure freedom for a minimum of 48 h to obtain interictal images.

Twenty-eight voluntary HCs without any history of febrile seizures, family history of epilepsy, neurologic or psychiatric disorders were recruited by taking into consideration similar mean age and educational years and gender distribution of both groups.

The study was approved by the Ethics Committee and was conducted in accordance with the Declaration of Helsinki. Written informed consent was obtained from all participants, or from the parents of participants who were younger than 18 years.

### 2.2. MRI data acquisition

MRI data were acquired on a 3 T scanner (Philips Achieva, Best, The Netherlands) with a 32-channel head coil. High resolution T1-weighted structural 3D images were acquired with the following parameters: repetition time/echo time (TR/TE): 8.4/3.9 ms, flip angle: 8°, field of view (FOV): 250 × 250 mm, 180 axial slices and 1 $mm^3$ voxel size.

Resting-state fMRI data were obtained using an echo planar images (EPI) sequence with the following parameters: TR: 2 s, TE: 30 ms, flip angle: 77°, FOV: 224 × 240 mm, acquisition matrix size: $^{11}2 \times 117$ and voxel size: 2 × 2 × 4 $mm^3$ in-plane resolution. Following 10 dummy volumes, 214 volumes each containing 36 axial slices covering the whole brain, were obtained with a total scan time of 448 s. All participants were instructed to remain awake and lie in the most relaxed position with closed eyes, and not to focus on anything in particular. MRI data of all patients were performed while they were taking their usual antiepileptic treatments.

### 2.3. fMRI data preprocessing

The data were preprocessed using CONN functional connectivity toolbox version 18.b (https://www.nitrc.org/projects/conn) (Whitfield-Gabrieli and Nieto-Castanon, 2012 and Nieto-Castanon, 2020) and SPM 12 (Statistical Parametric Mapping version 12; http://www.fil.ion.ucl.ac.uk/spm/). First, the functional images were realigned to the first image in order to correct for head motion. Then the Artifact Detection Tools (ART) toolbox (https://www.nitrc.org/projects/artifact_detect) implemented in CONN's preprocessing pipeline was used for identification of outlier scans in terms of excessive subject motion and signal intensity spikes. The global-signal (GS) z-value threshold for signal intensity outliers was set at 5 standard deviations (SD) greater than or less than the mean intensity of the entire session, and the threshold value for difference in composite motion of an image was set as 0.9 mm or greater from the previous scan. Two participants in the JME group with outliers more than 20% (>43) of the total number of functional volumes (214) were excluded from further analysis. Afterwards, functional and structural data were coregistered. Then, the structural images were segmented into white matter (WM), gray matter, and cerebrospinal fluid (CSF), and normalized to the Montreal Neurological Institute (MNI) standard space. Using the resulting transformation matrix, the functional data were spatially normalized and resampled to 2 $mm^3$ voxels. Finally, the functional data were smoothed by spatial convolution with an isotropic Gaussian kernel (full width half maximum = 8 mm).

Additionally, we undertook several extra steps to account for head motion. First, mean frame-wise displacement (FD) of functional images was calculated (Power et al., 2012). Afterwards, mean FD, number of outlier scans, mean GS change and mean motion were compared between whole JME group (JME-PS and JME-NPS) and HCs with two-samples t tests. There were no significant differences in mean FD ($t(55) = 0.694$, $p = 0.491$), number of outlier scans ($t(55) = -0.703$, $p = 0.485$), mean GS change ($t(55) = 0.105$, $p = 0.917$) and mean motion ($t(55) = 0.603$, $p = 0.549$). Then, these parameters were compared among JME-PS, JME-NPS and HC groups with one way ANOVA. There were also no significant differences in mean FD ($F(2,54) = 0.841$, $p = 0.437$), number of outlier scans ($F(2,54) = 0.634$, $p = 0.534$), mean GS change ($F(2,54) = 0.240$, $p = 0.787$) and mean motion ($F(2,54) = 0.977$, $p = 0.383$). The mean motion values for each group were as follows: whole JME group = 0.15 ± 0.07, JME-PS group = 0.14 ± 0.05, JME-NPS group = 0.17 ± 0.09 and HC group = 0.14 ± 0.06.

### 2.4. Functional connectivity analyses

Seed-to-voxel FC analysis was performed using the CONN toolbox.

A total of 25 seeds were used for the analysis. Right and left intracalcarine cortices, occipital poles and thalami were defined based on the FSL Harvard-Oxford Atlas which is implemented in CONN. Thalamic seeds were defined based on the histological atlas by Krauth et al. (2010) and seeds to characterize the ARAS were defined based on the Harvard Ascending Arousal Network Atlas, including main investigated nuclei forming the ARAS (Edlow et al., 2012). The selected seeds/regions of interest (ROIs) are summarized in Table 1.

First, in order to remove physiological noise from the blood oxygen dependent level (BOLD) signal, additional preprocessing steps were performed on the functional images. CONN's denoising procedure was applied on the functional data to remove effects of potential noise sources involving movement and physiological effects. The denoising pipeline includes linear regression of potential noise effects in the BOLD signal as well as application of temporal band-pass filter (Nieto-Castanon, 2020). The identified potential noise effects are estimated for each voxel and removed with the linear regression procedure (Nieto-Castanon, 2020). In this step, CONN uses an anatomical component based noise correction (aCompCor) method instead of removal of GS (Behzadi et al., 2007). With this procedure, potential noise components derived from WM and CSF signals were estimated and included as confounds in the denoising step. Six subject motion parameters (three translation and three rotation) obtained in the realignment step and their first order derivatives resulting in a total of twelve motion components per subject were also added. Furthermore, outlier scans of subjects defined with ART in the preprocesssing step were included as potential noise effects. Finally, effect of the scanning session was included into confounding effects in order to decrease the influence of slow, linear trends in BOLD signal (Nieto-Castanon, 2020). Then bandpass filter of 0.01−0.1 Hz was applied to the functional images in order to filter effects from noise sources.

**Table 1**
Selected ROIs.

| | |
|---|---|
| ■ Intracalcarine cortex R & L | ■ ARAS seeds: |
| ■ Occipital pole R & L | Median raphe (MR) |
| ■ Thalamus R & L | Dorsal raphe (DR) |
| ■ Pulvinar R & L | Locus coeruleus (LC) |
| ■ Posterior nuclei of thalamus≠ R & L | Mesencephalic reticular formation (MRF) |
| ■ Lateral geniculate nucleus R & L | Parabrachial complex (PBC) |
| ■ Central median nucleus R & L | Periaqueductal gray area (PAG) |
| ■ Central lateral nucleus R & L | Pontine oralis (PO) |
| | Pedinculopontine nucleus (PPN) |
| | Ventral tegmental area (VTA) |

≠According to Krauth's atlas, the thalamic nuclei forming the posterior group are as follows: medial/inferior/lateral/anterior pulvinar, lateral posterior nucleus, medial geniculate nucleus, suprageniculate nucleus, limitans nucleus, posterior nucleus, lateral geniculate nucleus.
ROIs: Regions of interest, ARAS: Ascending reticular activating system. R: Right, L: Left.

Subject level FC analysis was performed by calculating the bivariate correlation coefficients between the average time course for each seed using unsmoothed data with the time courses of all other voxels in the brain using smoothed data. All correlation values were transformed using Fisher's z-transformation. The group comparisons were first performed between the whole JME group and HCs. Then, three pairwise comparisons were conducted among the JME-PS, JME-NPS and HC groups. For all subgroup comparisons, the same HC group comprising 28 subjects was used.

Results at voxel-level height threshold $p < 0.001$ (uncorrected) combined with a cluster level family-wise error (FWE) corrected threshold $p_{FWE\text{-}corr} < 0.002$ (0.05/25) (Bonferroni corrected for number of seeds) were reported.

### 2.5. Clinical data analyses

SPSS package (IBM SPSS Statistics for Windows, Version 21.0) was used for statistical analyses. Shapiro-Wilk normality test was used to test the normality of the distribution of quantitative data between groups. The independent samples *t*-test and one-way ANOVA were used to compare normally distributed continuous variables, whereas the Mann-Whitney *U* test and Kruskal-Wallis H test were used for variables not normally distributed. Pearson's chi-square test was used to compare categorical variables, and the significance level was accepted as $p < 0.05$.

## 3. Results

### 3.1. Clinical characteristics

The cohort comprised of 29 patients (16 JME-PS and 13 JME-NPS) and 28 HCs (Table 2).

Over half of the patients (n = 17) patients were taking valproate (58.6%) and were under monotherapy (JME-PS: 81.3% (n = 12) / JME-NPS: 69.2% (n = 5). There was no difference in terms of seizure control between the subgroups of JME ($p$=0.956).

**Table 2**
The demographics of the study groups.

| | a) | | | | b) | | | | |
|---|---|---|---|---|---|---|---|---|---|
| | JME (N = 29) | HC (N = 28) | Test | *p* | JME-PS (N = 16) | JME-NPS (N = 13) | HC (N = 28) | Test | *p* |
| **Age (Mean ± SD)** | 27.3 ± 7.24 | 31.29 ± 8.35 | $t(55) = 1.890$ | 0.064[e] | 27.06 ± 6.53 | 27.7 ± 8.30 | 31.29 ± 8.35 | $F(2) = 1.783$* | 0.178[a] |
| **Gender (F/M ratio)** | 17/12 | 14/14 | $\chi^2(1) = 0.150$ | 0.699[b] | 12/4 | 5/8 | 14/14 | $\chi^2(2) = 4.287$ | 0.117[b] |
| **Years of education (Mean ± SD)** | 10.97 ± 4.28 | 12.36 ± 4.87 | $U(55) = 364.50$ | 0.504[d] | 10.88 ± 4.60 | 11.08 ± 4.05 | 12.36 ± 4.87 | $\chi^2(2) = 0.446$* | 0.800[c] |
| **Age of seizure onset (Mean ± SD)** | 14.04 ± 4.69 | – | – | – | 15 ± 4.60 | 12.75 ± 4.69 | – | $U(27) = 84$ | 0.575[d] |
| **Duration of disease (Mean ± SD)** | 13.14 ± 8.95 | – | – | – | 12.06 ± 6.59 | 14.58 ± 11.56 | – | $t(27) = 0.731$ | 0.471[e] |

a) Indicates that comparison of all JME patients with HC, b) Indicates that comparison of JME-PS, JME-NPS and HC.
JME: Juvenile myoclonic epilepsy, HC: Healthy control, JME-PS: Photosensitive juvenile myoclonic epilepsy, JME-NPS: Non-photosensitive juvenile myoclonic epilepsy, SD: Standard deviation, F: Female, M:Male,[a] One Way ANOVA, [b]Pearson's chi-square test [c] Kruskal-Wallis H test, [d]Mann-Whitney *U* test, [e]Independent samples *t*-test.
* In addition, pairwise comparisons were also made between the JME-PS vs HC, JME-NPS vs HC and JME-PS vs JME-NPS groups, and no significant difference was found.

### 3.2. fMRI findings

Seed-to-voxel resting-state FC analyses were conducted for following subgroups: the whole JME (N = 29) vs. all HC (N = 28); JME-PS (N = 16) vs JME-NPS (N = 13); JME-PS (N = 16) vs all HC (N = 28); JME-NPS (N = 13) vs all HC (N = 28). These FC analyses revealed significant differences among the groups for 3 of the 25 seeds including MRF, locus coeruleus and right posterior nuclei of the thalamus.

MRF seed revealed significant hyperconnectivity with the bilateral paracingulate gyrus and anterior cingulate cortex i) in the whole JME group compared to HCs ($p_{FWE\text{-}corr} = 0.000000019$) (Fig. 1A), ii) in the JME-PS group compared to HCs ($p_{FWE\text{-}corr} = 0.000018$) (Fig. 1B) and iii) in the JME-NPS group compared to HCs ($p_{FWE\text{-}corr} = 0.0019$) (Fig. 1C).

Locus coeruleus seed displayed significant hyperconnectivity in JME-PS group compared to HCs with a cluster corresponding to the bilateral lingual gyri, intracalcarine cortices, occipital poles and left occipital fusiform gyrus ($p_{FWE\text{-}corr} = 0.000000000019$) (Fig. 2A). Additionally, locus coeruleus seed showed significant hyperconnectivity in JME-PS group compared to JME-NPS group with a cluster corresponding to the bilateral lingual gyri and right intracalcarine cortex ($p_{FWE\text{-}corr} = 0.00029$) (Fig. 2B).

Lastly, the right posterior nuclei of thalamus revealed significant hyperconnectivity in JME-PS group compared to HCs with a cluster corresponding to the right superior lateral occipital cortex ($p_{FWE\text{-}corr} = 0.0012$) (Fig. 3). We did not find a significant connectivity difference of the left posterior thalamic nuclei. There were no other FC changes between ARAS and other brain regions including the motor cortices. The significant results are summarized in Table 3.

## 4. Discussion

This study demonstrates, for the first time, increased FC between the MRF and the bilateral paracingulate gyrus and anterior cingulate cortex in JME compared to HCs. In addition, we found increased FC of locus coeruleus with primary visual areas, in JME-PS group compared to JME-NPS and HCs.

### 4.1. Altered functional connectivity of ARAS in JME

A recent rs-fMRI/DTI study reported disruptions in the connectivity between ARAS and mainly neocortical regions suggesting that these changes might be related to cognitive and psychosocial interictal problems seen in patients with temporal lobe epilepsy (TLE) (Englot et al., 2018). Another rs-fMRI study further showed increased FC between ARAS and thalamus in preoperative patients with TLE and abnormal brainstem-thalamus connectivity was found to be associated with impaired visual attention (González et al., 2019). The current study reveals and describes increased FC of ARAS in JME syndrome.

We found significant hyperconnectivity of MRF with the bilateral paracingulate gyrus and anterior cingulate cortex in the both JME groups. MRF is well known to be associated with consciousness and sleep-wake cycles among ARAS structures whereas cingulate cortex is mainly associated with affective and cognitive functions regulating the frontothalamic circuit (Cao et al., 2013; Basta and Cascella, 2020; Fornito et al., 2004). The role of anterior cingulate and paracingulate cortices in directing attention during visual cognitive tests has been demonstrated in a recent task-based fMRI study (Gennari et al., 2018). Perhaps altered FC between the MRF and both the anterior cinculate and paracingulate cortices underlies cognitive and emotional impairments and triggers for seizures in JME. Interictal cognitive and emotional problems have been described in JME (Zamarian et al., 2013). A meta-analysis study also reported increased gray matter volumes in the anterior cingulate cortex in JME (Cao et al., 2013). Furthermore, increased BOLD activity has been reported in the anterior cingulate gyrus at the beginning of GSWDs in patients with GGEs (Benuzzi et al., 2012).

The locus coeruleus plays a role in alertness and "awakening" reactions of the ARAS and has widespread connections with various cortical and subcortical structures (Arguinchona and Tadi, 2020; Zhang et al., 2016). We found increased FC of locus coeruleus with the bilateral lingual gyri, intracalcarine cortices, occipital poles and left occipital fusiform gyrus in JME-PS. Moreover, increased connectivity of locus coeruleus was seen with the bilateral lingual gyri and right intracalcarine cortex in the JME-PS compared to the JME-NPS group. Perhaps the increased functional connectivity between the locus coeruleus and visual cortex demonstrated in this study contributes to seizures triggered by awakening and light stimulation.

Experimental studies have highlighted the role of the locus coeruleus in the pathogenesis of epilepsy. A rat kindling study revealed that seizure suppression could be achieved by destroying locus coeruleus neurons (Lindvall et al., 1988). Structural and functional connectivity studies are needed to elucidate the role of locus ceruleus in the pathophysiology of JME.

### 4.2. Altered functional connectivity of posterior thalamus

We investigated the FC differences of the entire thalamus and also focused on pulvinar and lateral geniculate nucleus (LGN) as they have key roles for the visual neural networks (Krauth et al., 2010; Schmid et al., 2010; Krueger and Disney, 2019; Benarroch, 2015).

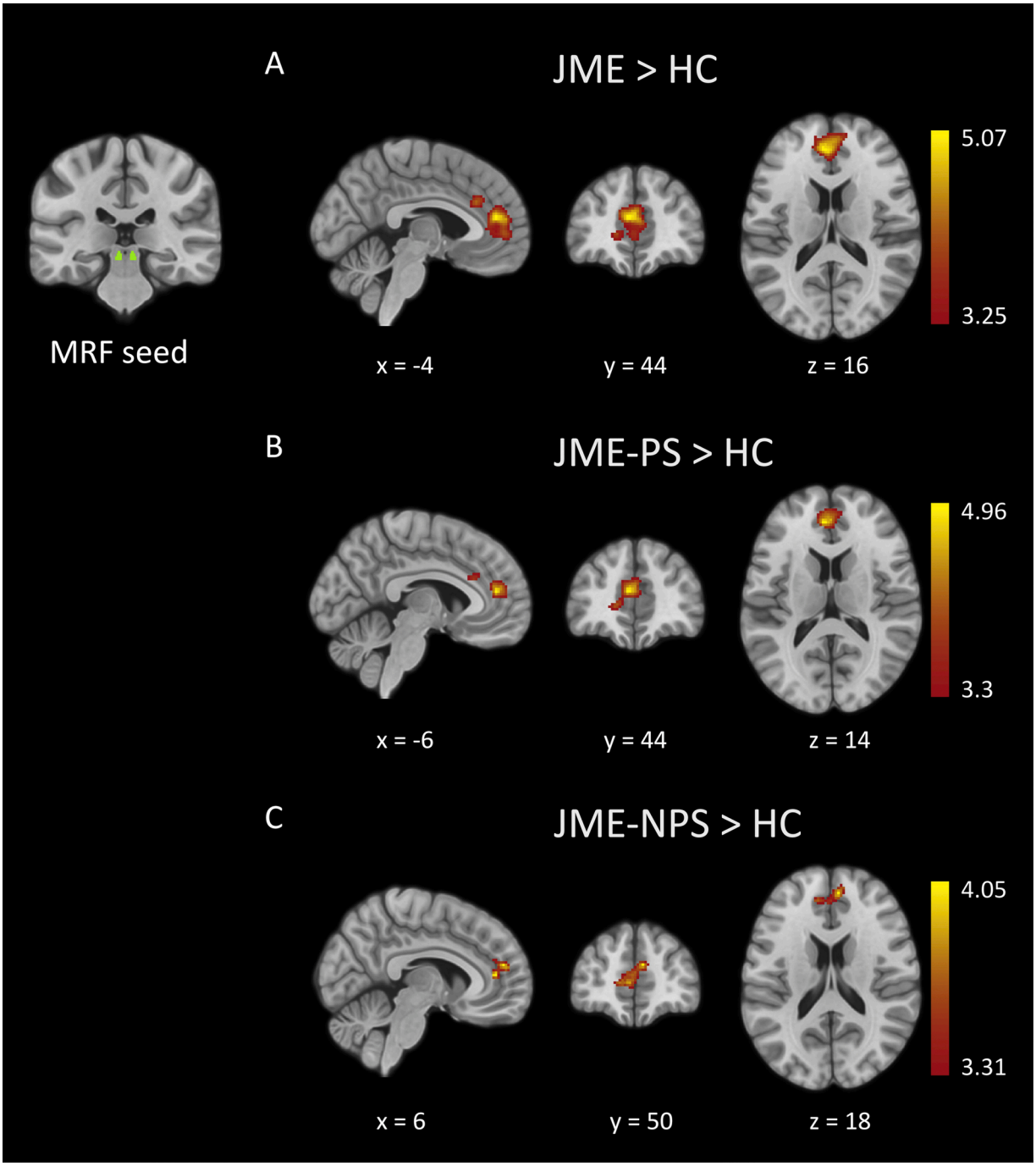



**Fig. 1.** Hyperconnectivity of mesencephalic reticular formation (MRF). For the MRF seed, (A) whole JME group (N = 29) (cluster size: 1173 voxels; $p_{FWE\text{-}corr} < 0.001$), B) JME-PS group (N = 16) (cluster size: 608 voxels; $p_{FWE\text{-}corr} < 0.001$) and C) JME-NPS group (N = 13) (cluster size: 326 voxels; $p_{FWE\text{-}corr} = 0.002$) displayed increased functional connectivity with the bilateral paracingulate gyrus and anterior cingulate cortex in comparison to the HCs (N = 28). Color maps represent the *t* values.

Wang et al. (2012) showed that the gray matter volumes of pulvinar nuclei decreased in GGE with generalized tonic-clonic seizures, but they could not show a significant difference in the connectivity of the pulvinar. We did not find an altered FC of pulvinar, either. Conversely, Vaudano et al. (2017) reported that the connectivity of pulvinar with somatosensory and visual cortices was decreased in GGEs with photosensitivity. However, the majority of their study population was composed of patients with eyelid myoclonia. Therefore, one possible explanation for the discrepancy between the findings of the studies may relate to this syndromic difference.

In our study, the FC between the right posterior thalamus and the the right lateral occipital cortex was found to be increased, particularly in PS-JME patients. Thus, altered light perception may play a role in the pathogenesis of seizures after morning awakening and also by light exposure in JME. Perhaps the increased connectivity of the right rather than left thalamus relates to relative hemispheric dominance of visual processing.

LGN receives varying degrees of regulatory inputs from ARAS structures including locus coeruleus (Schmid et al., 2010; Krueger and Disney, 2019). In LGN kindling rats, similar to patients with PS epilepsy, changes of visual evoked potentials have been demonstrated (Ishikawa et al., 2008). The role of LGN in JME has not been studied much, so far.

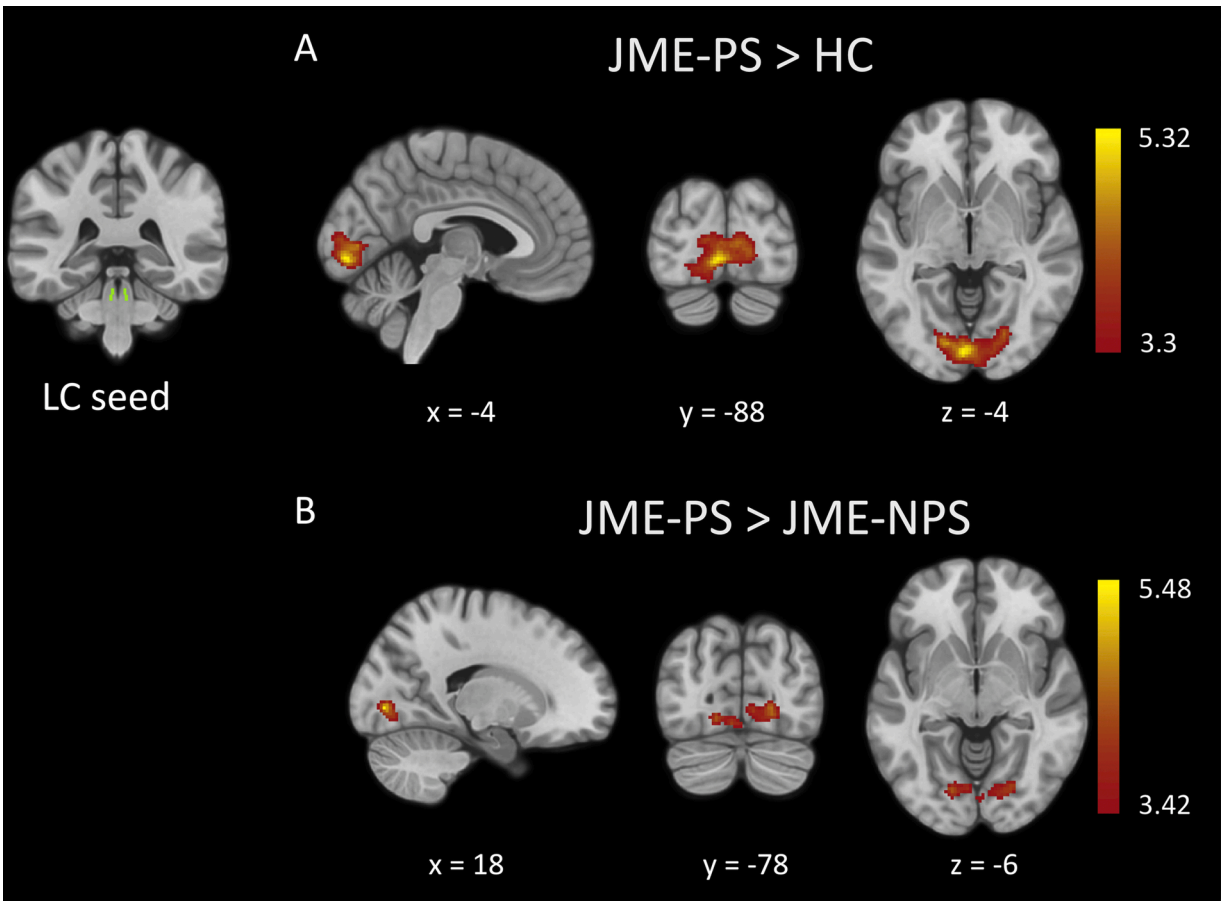



**Fig. 2.** Hyperconnectivity of locus coeruleus (LC). For the LC seed, the JME-PS group (N = 16) showed increased functional connectivities with the bilateral lingual gyri, intracalcarine cortices, occipital poles and left occipital fusiform gyrus compared to HCs (N = 28) (cluster size: 1671 voxels; $p_{FWE\text{-}corr} < 0.001$) and B) with the bilateral lingual gyri and right intracalcarine cortex compared to JME-NPS group (N = 13) (cluster size: 400 voxels; $p_{FWE\text{-}corr} < 0.001$). Color maps represent the *t* values.

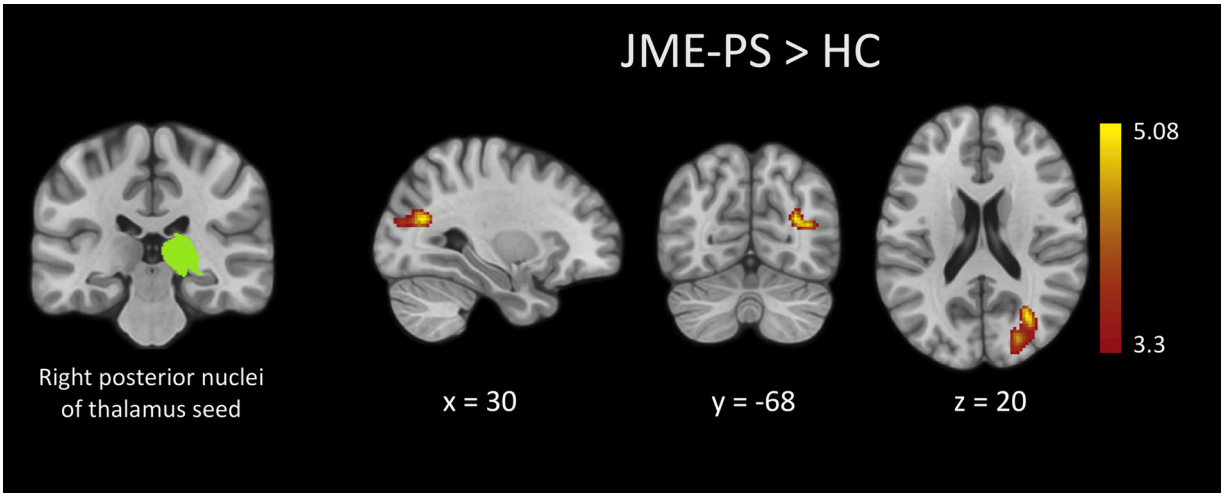



**Fig. 3.** Hyperconnectivity of the right posterior nuclei of thalamus. For the right posterior nuclei of thalamus seed, JME-PS group (N = 16) displayed increased functional connectivity with right superior lateral occipital cortex compared to HCs (N = 28) (cluster size: 385 voxels; $p_{FWE\text{-}corr} < 0.002$). Color maps represent the *t* values.

In a recent small-sized DTI study, a reduction in fractional anisotropy has been revealed in LGN among the whole JME group suggesting that these microstructural abnormalities seen in LGN could also be associated with seizures upon awakening in patients with JME (von Podewils et al., 2015). We could not localize the increased FC of the posterior thalamus to the LGN; perhaps

LGN might be one of the responsible structures for the increased connectivity of posterior thalamus observed in our JME patients with photosensitivity.

**Table 3**
Seed-to-voxel functional connectivity results at height threshold $p < 0.001$ (uncorrected) combined with cluster level threshold $p_{FWE\text{-}corr} < 0.002$ (Bonferroni corrected for multiple comparisons [number of seeds = 25]).

| Seed Region | Regions showing connectivity changes | Group contrast | Cluster size | Peak coordinate (x y z) | $T_{max}$ | $p_{FWE\text{-}corr}$ | Effect size (Cohen's d) |
|---|---|---|---|---|---|---|---|
| MRF | Bilateral paracingulate gyri, ACC | JME > HC | 1173 | −4 44 16 | 5.07 | < 0.001 | 1.37 |
| | Bilateral paracingulate gyri, ACC | JME-PS > HC | 608 | −6 44 14 | 4.96 | < 0.001 | 1.53 |
| | Bilateral paracingulate gyri, ACC | JME-NPS > HC | 326 | 6 50 18 | 4.05 | 0.002 | 1.30 |
| LC | Bilateral lingual gyri, intracalcarine cortices, occipital poles, Left occipital fusiform gyrus | JME-PS > HC | 1671 | −18 -82 -08 | 5.32 | < 0.001 | 1.64 |
| | Bilateral lingual gyri, Right intracalcarine cortex | JME-PS > JME-NPS | 400 | 18 -82 0 | 5.48 | < 0.001 | 2.11 |
| Right posterior nuclei of thalamus | Right superior lateral occipital cortex | JME-PS > HC | 385 | 30 -68 20 | 5.08 | < 0.002 | 1.57 |

MRF: Mesencephalic reticular formation, LC: Locus coeruleus, ACC: Anterior cingulate cortex, JME: Juvenile myoclonic epilepsy, HC: Healthy control, JME-PS: Photosensitive juvenile myoclonic epilepsy, JME-NPS: Non-photosensitive juvenile myoclonic epilepsy, x: Sagittal, y: Coronal, z: Axial coordinates.

### *4.3. Functional connectivity of primary visual areas*

Previous studies consistently supported the existence of a pathway between the visual and motor networks (Artieda and Obeso, 1993; Cantello et al., 2000; Strigaro et al., 2015a). Another fMRI study proposed that repetitive intermittent light stimulation caused excessive neural activity in the visual cortex, resulting in photoparoxysmal EEG response and consequently, generalized tonic-clonic seizures (Moeller et al., 2009). On the other hand, it has been reported that baboons with photosensitivity showed strong activation in the right anterior cingulate while the activation in the occipital cortex was strikingly absent by positron emission tomography (PET) imaging during intermittent light stimulation (Szabó et al., 2011). Strigaro et al. (2015b) demonstrated that photosensitive patients with GGE responded to impulses from the visual cortex excessively in the motor cortex by a transcranial magnetic stimulation (TMS) study. Thus, this increased response could explain the spread of photoparoxysmal response to the front, hence the development of motor activity such as myoclonia.

The increased connectivity between occipital lobe and SMA was reported to be notable in JME-PS patients by DTI and fMRI, but not significantly (Vollmar et al., 2012). Based on the previous data, we had expected an altered connectivity of visual cortical areas in JME-PS compared to JME-NPS. However, we could not show a significant difference for these subgroups. The potential effects of antiepileptic drugs should be considered, when evaluating FC changes. Over half of our patients were taking valproate. Results of an fMRI study in patients with JME showed that valproate decreased the excessive FC between the parieto-frontal and motor networks (Vollmar et al., 2011). Moreover, in the baboon model of GGE, reduced FC in primary visual and parietal neural networks has been shown after the administration of valproate. (Salinas and Szabó, 2017). Recently, in patients with epilepsy using valproate, Tondelli et al. (2020) reported reduced cortical thickness in the posterior cortex, particularly in the visual cortex. Thus, drug treatment might have covered FC changes of the visual cortex in our study.

## 5. Conclusion

Our study is important in terms of showing altered FC of ARAS by rs-fMRI in JME for the first time. We also disclosed connectivity differences of visual networks when comparing PS and NPS subgroups of JME.

The limitations of our single-center study include the usage of antiepileptic drugs for ethical reasons, the relatively low number of patients, and heterogeneous seizure frequency and disease duration.

Further simultaneous EEG-fMRI studies can provide additional information regarding the possibility of effects of GSWDs at the time of EEG recordings. Given the seizures' triggers are invaluable clues, investigating endophenotypes in JME, may shed light on the unknown epileptogenic mechanisms to develop individual paradigms for seizure prevention.

## Contributors

Conception and design of the study: EUO, TD and BB. Acquisition and analysis of data: EUO, EK, NGS, NB, EH, KE, CUY. Drafting the manuscript and figures: EUO, EK, UA and BB. Revising the manuscript for intellectual content: EK, NGS, EH, UA, NB, TD and BB.

## Declaration of competing interest

None of the authors have any conflicts of interest to disclose. We confirm that we have read the Journal's position on issues involved in ethical publication and affirm that this report is consistent with those guidelines.

## Acknowledgments

We would like to thank Dr. Daniel Major for his careful proofreading.

This study was supported by Istanbul University Scientific Research Projects Unit (Projects ID/number: TYL-25538).

## References

Aghakhani, Y., Bagshaw, A.P., Bénar, C.G., Hawco, C., Andermann, F., Dubeau, F., et al., 2004. fMRI activation during spike and wave discharges in idiopathic generalized epilepsy. Brain 127, 1127–1144. https://doi.org/10.1093/brain/awh136.

Arguinchona, J.H., Tadi, P., 2020. Neuroanatomy, reticular activating system. StatPearls. StatPearls Publishing, Treasure Island (FL), p. 2020. Last update: July 31. https://www.ncbi.nlm.nih.gov/books/NBK549835.

Artieda, J., Obeso, J.A., 1993. The pathophysiology and pharmacology of photic cortical reflex myoclonus. Ann. Neurol. 34, 175–184. https://doi.org/10.1002/ana.410340213.

Badawy, R.A., Macdonell, R.A., Jackson, G.D., Berkovic, S.F., 2009. Why do seizures in generalized epilepsy often occur in the morning? Neurology 73 (3), 218–222. https://doi.org/10.1212/WNL.0b013e3181ae7ca6.

Bartolini, E., Pesaresi, I., Fabbri, S., Cecchi, P., Giorgi, F.S., Sartucci, F., et al., 2014. Abnormal response to photic stimulation in juvenile myoclonic epilepsy: an EEG-fMRI study. Epilepsia 55 (7), 1038–1047. https://doi.org/10.1111/epi.12634.

Basta, M., Cascella, M., 2020. Neuroanatomy, mesencephalon midbrain. StatPearls. StatPearls Publishing, Treasure Island (FL), p. 2020. Last update: May 2. https://www.ncbi.nlm.nih.gov/books/NBK551509/.

Baykan, B., Wolf, P., 2017. Juvenile myoclonic epilepsy as a spectrum disorder: a focused review. Seizure 49, 36–41. https://doi.org/10.1016/j.seizure.2017.05.011.

Behzadi, Y., Restom, K., Liau, J., Liu, T.T., 2007. A component based noise correction method (CompCor) for BOLD and perfusion based fMRI. Neuroimage 37, 90–101. https://doi.org/10.1016/j.neuroimage.2007.04.042.

Benarroch, E.E., 2015. Pulvinar: associative role in cortical function and clinical correlations. Neurology 84, 738–747. https://doi.org/10.1212/WNL.0000000000001276.

Benuzzi, F., Mirandola, L., Pugnaghi, M., Farinelli, V., Tassinari, C.A., Capovilla, G., et al., 2012. Increased cortical BOLD signal anticipates generalized spike and wave

discharges in adolescents and adults with idiopathic generalized epilepsies. Epilepsia 53, 622–630. https://doi.org/10.1111/j.15281167.2011.03385x.
Brigo, F., Bongiovanni, L.G., Nardone, R., Trinka, E., Tezzon, F., Fiaschi, A., et al., 2013. Visual cortex hyperexcitability in idiopathic generalized epilepsies with photosensitivity: a TMS pilot study. Epilepsy Behav. 27 (2), 301–306. https://doi.org/10.1016/j.yebeh.2013.02.010.
Cantello, R., Civardi, C., Cavalli, A., Varrasi, C., Vicentini, R., 2000. Effects of a photic input on the human cortico-motoneuron connection. Clin. Neurophysiol. 111, 1981–1989. https://doi.org/10.1016/S1388-2457(00)00431-4.
Cao, B., Tang, Y.Y., Li, J.P., Zhang, X., Shang, H.F., Zhou, D., 2013. A meta-analysis of voxel-based morphometry studies on gray matter volume alteration in juvenile myoclonic epilepsy. Epilepsy Res. 106, 370–377. https://doi.org/10.1016/j.eplepsyres.2013.07.003.
Edlow, B.L., Takahashi, E., Wu, O., Benner, T., Dai, G., Bu, L., et al., 2012. Neuroanatomic connectivity of the human ascending arousal system critical to consciousness and its disorders. J. Neuropathol. Exp. Neurol. 71 (6), 531–546. https://doi.org/10.1097/NEN.0b013e3182588293.
Englot, D.J., Gonzalez, H., Reynolds, B.B., Konrad, P.E., Jacobs, M.L., Gore, J., et al., 2018. Relating structural and functional brainstem connectivity to disease measures in epilepsy. Neurology 91 (1), e67–e77. https://doi.org/10.1212/WNL.0000000000005733.
Fornito, A., Yücel, M., Wood, S., Stuart, G.W., Buchanan, J.A., Proffitt, T., et al., 2004. Individual differences in anterior cingulate/paracingulate morphology are related to executive functions in healthy males. Cereb. Cortex 14, 424–431. https://doi.org/10.1093/cercor/bhh004.
Gennari, S.P., Millman, R.E., Hymers, M., Mattys, S.L., 2018. Anterior paracingulate and cingulate cortex mediates the effects of cognitive load on speech sound discrimination. Neuroimage 178, 735–743. https://doi.org/10.1016/j.neuroimage.2018.06.035.
Gloor, P., 1968. Generalized Cortico-Reticular Epilepsies Some Considerations on the Pathophysiology of Generalized Bilaterally Synchronous Spike and Wave Discharge. Epilepsia 9, 249–263. https://doi.org/10.1111/j.1528-1157.1968.tb04624.x.
González, H.F.J., Chakravorti, S., Goodale, S.E., Gupta, K., Claassen, D.O., Dawant, B., et al., 2019. Thalamic arousal network disturbances in temporal lobe epilepsy and improvement after surgery. J. Neurol. Neurosurg. Psychiatry. 90 (10), 1109–1116. https://doi.org/10.1136/jnnp-2019-320748.
Hamandi, K., Salek-Haddadi, A., Laufs, H., Liston, A., Friston, K., Fish, D.R., et al., 2006. EEG-fMRI of idiopathic and secondarily generalized epilepsies. Neuroimage 31 (4), 1700–1710. https://doi.org/10.1016/j.neuroimage. 2006.02.016.
Hashizume, K., Tanaka, T., Fujita, T., Tanaka, S., 2000. Generalized seizures induced by an epileptic focus in the mesencephalic reticular formation: impact on the understanding of the generalizing mechanism. Stereotact. Funct. Neurosurg. 74, 153–160. https://doi.org/10.1159/000056474.
Hill, R.A., Chiappa, K.H., Huang-Hellinger, F., Jenkins, B.G., 1999. Hemodynamic and metabolic aspects of photosensitive epilepsy revealed by functional magnetic resonance imaging and magnetic resonance spectroscopy. Epilepsia 40 (7), 912–920. https://doi.org/10.1111/j.1528.
Holmes, M.D., Quiring, J., Tucker, D.M., 2010. Evidence that juvenile myoclonic epilepsy is a disorder of fronto- temporal corticothalamic networks. Neuroimage 49, 80–93. https://doi.org/10.1016/j.neuroimage.2009.08.04.
Ishikawa, T., Fujiwara, A., Takechi, K., Ago, J., Matsumoto, N., Rahman, M.A., et al., 2008. Changes of visual evoked potential induced by lateral geniculate nucleus kindling in rats. Epilepsy Res. 79, 146–150. https://doi.org/10.1016/j.eplepsyres.2008.01.001.
Jang, S.H., Kwon, H.G., 2015. The direct pathway from the brainstem reticular formation to the cerebral cortex in the ascending reticular activating system: a diffusion tensor imaging study. Neurosci. Lett. 8 (606), 200–203. https://doi.org/10.1016/j.neulet.2015.09.004.
Jiang, S., Luo, C., Liu, Z., Hou, C., Wang, P., Dong, L., et al., 2016. Altered local spontaneous brain activity in juvenile myoclonic epilepsy: a preliminary resting-state fMRI study. Neural Plast. 1–7. https://doi.org/10.1155/2016/3547203.
Krauth, A., Blanc, R., Poveda, A., Jeanmonod, D., Morel, A., Székely, G., 2010. A mean three-dimensional atlas of the human thalamus: generation from multiple histological data. Neuroimage 49, 2053–2062. https://doi.org/10.1016/j.neuroimage.2009.10.042.
Krueger, J., Disney, A.A., 2019. Structure and function of dual-source cholinergic modulation in early vision. J. Comp. Neurol. 527 (3), 738–750. https://doi.org/10.1002/cne.24590.
Li, R., Hu, C., Wang, L., Liu, D., Liu, D., Liao, W., et al., 2020. Disruption of functional connectivity among subcortical arousal system and cortical networks in temporal lobe epilepsy. Brain Imaging Behav. 14 (3), 762–771. https://doi.org/10.1007/s11682-018-0014-y.
Lindvall, O., Kikvadze, I., Brundin, P., Björklund, A., Barry, D.I., Bolwig, T.G., 1988. Intracerebral grafting of fetal noradrenergic locus coeruleus neurons: Evidence for seizure suppression in the kindling model of epilepsy. Prog. Brain Res. 78, 79–86. https://doi.org/10.1016/S0079-6123(08)60269-1.
Moeller, F., Siebner, H.R., Wolff, S., Muhle, H., Granert, O., Jansen, O., et al., 2009. Mapping brain activity on the verge of a photically induced generalized tonic–clonic seizure. Epilepsia 50 (6), 1632–1637. https://doi.org/10.1111/j.1528-1167.2009.02011.x.
Nieto-Castanon, A., 2020. Handbook of Functional Connectivity Magnetic Resonance Imaging Methods in CONN. Hilbert Press, Boston.
Paus, T., 2000. Functional anatomy of arousal and attention systems in the human brain. Prog. Brain Res. 126, 65–77. https://doi.org/10.1016/S0079-6123(00)26007-X.
Pellegrini, A., Ermani, M., Testa, G., 1985. Involvement of cortical, thalamic and midbrain reticular formation neurons in spike and wave discharges: extracellular study in feline generalized penicillin epilepsy. Exp. Neurol. 89 (2), 465–478. https://doi.org/10.1016/0014-4886(85)90106-2.
Power, J.D., Barnes, K.A., Snyder, A.Z., Schlaggar, B.L., Petersen, S.E., 2012. Spurious but systematic correlations in functional connectivity MRI networks arise from subject motion. Neuroimage 59 (3), 2142–2154. https://doi.org/10.1016/j.neuroimage.2011.10.018.
Salinas, F.S., Szabó, C.Á., 2017. Resting-state functional connectivity changes due to acute and short-term valproic acid administration in the baboon model of GGE. Neuroimage Clin. 16, 132–141. https://doi.org/10.1016/j.nicl.2017.07.013.
Scheffer, I.E., Berkovic, S., Capovilla, G., Connolly, M.B., French, J., Guilhoto, L., et al., 2017. ILAE classification of the epilepsies: position paper of the ILAE commission for classification and terminology. Epilepsia 58, 512–521. https://doi.org/10.1111/epi.13709.
Schmid, M.C., Mrowka, S.W., Turchi, J., Saunders, R.C., Wilke, M., Peters, A.J., et al., 2010. Blindsight depends on the lateral geniculate nucleus. Nature 466, 373–377. https://doi.org/10.1038/nature09179.
Strigaro, G., Ruge, D., Chen, J.C., Marshall, L., Desikan, M., Cantello, R., Rothwell, J.C., 2015a. Interaction between visual and motor cortex: A transcranial magnetic stimulation study. J. Physiol. (Paris) 593, 2365–2377. https://doi.org/10.1113/JP270135.
Strigaro, G., Falletta, L., Varrasi, C., Rothwell, J.C., Cantello, R., 2015b. Overactive visuomotor connections underlie the photoparoxysmal response. A TMS study. Epilepsia 56, 1828–1835. https://doi.org/10.1111/epi.13190.
Szabó, C.Á., Salinas, F.S., Narayana, S., 2011. Functional PET evaluation of the photosensitive baboon. Open Neuroimag. J. 5, 206–215. https://doi.org/10.2174/1874440001105010206.
Tondelli, M., Vaudano, A.E., Sisodiya, S.M., Meletti, S., 2020. Valproate use is associated with posterior cortical thinning and ventricular enlargement in epilepsy patients. Front. Neurol. 11, 622. https://doi.org/10.3389/fneur. 2020.00622.
Vaudano, A.E., Laufs, H., Kiebel, S.J., Carmichael, D.W., Hamandi, K., Guye, M., et al., 2009. Causal hierarchy within the thalamo-cortical network in spike and wave discharges. PLoS One 4 (8), e6475. https://doi.org/10.1371/journal.pone.0006475.
Vaudano, A.E., Ruggieri, A., Avanzini, P., Gessaroli, G., Cantalupo, G., Coppola, A., et al., 2017. Photosensitive epilepsy is associated with reduced inhibition of alpha rhythm generating networks. Brain. 140, 981–997. https://doi.org/10.1093/brain/awx009.
Vollmar, C., O'Muircheartaigh, J., Barker, G.J., Symms, M.R., Thompson, P., Kumari, V., et al., 2011. Motor system hyperconnectivity in juvenile myoclonic epilepsy: a cognitive functional magnetic resonance imaging study. Brain. 134, 1710–1719. https://doi.org/10.1093/brain/awr098.
Vollmar, C., O'Muircheartaigh, J., Symms, M.R., Barker, G.J., Thompson, P., Kumari, V., 2012. Altered microstructural connectivity in juvenile myoclonic epilepsy: the missing link. Neurology 78 (20), 1555–1559. https://doi.org/10.1212/WNL.0b013e3182563b44.
von Podewils, F., Runge, U., Krüger, S., Geithner, J., Wang, Z.I., Khaw, A.V., et al., 2015. Diffusion tensor imaging abnormalities in photosensitive juvenile myoclonic epilepsy. Eur. J. Neurol. 22 (8), 1192–1200. https://doi.org/10.1111/ene.12725.
Wang, Z., Zhang, Z., Jiao, Q., Liao, W., Chen, G., Sun, K., et al., 2012. Impairments of thalamic nuclei in idiopathic generalized epilepsy revealed by a study combining morphological and functional connectivity MRI. PLoS One 7 (7), e39701. https://doi.org/10.1371/journal.pone.0039701.
Whitfield-Gabrieli, S., Nieto-Castanon, A., 2012. Conn: a functional connectivity toolbox for correlated and anticorrelated brain networks. Brain Connect. 2 (3), 125–141. https://doi.org/10.1089/brain.2012.0073.
Wijdicks, E.F.M., 2019. The ascending reticular activating system. Neurocrit. Care 31 (2), 419–422. https://doi.org/10.1007/s12028-019-00687-7.
Xie, F., Xing, W., Wang, X., Liao, W., Shi, W., 2017. Altered states of consciousness in epilepsy: a DTI study of the brain. Int. J. Neurosci. 127 (8), 667–672. https://doi.org/10.1080/00207454.2016.1229668.
Zamarian, L., Höfler, J., Kuchukhidze, G., Delazer, M., Bonatti, E., Kemmler, G., et al., 2013. Decision making in juvenile myoclonic epilepsy. J. Neurol. 260, 839–846. https://doi.org/10.1007/s00415-012-6715-z.
Zeman, A., 2001. Consciousness. Brain 124 (Pt 7), 1263–1289. https://doi.org/10.1093/brain/124.7.1263.
Zhang, S., Hu, S., Chao, H.H., Li, C.S.R., 2016. Resting-State Functional Connectivity of the Locus Coeruleus in Humans: In Comparison with the Ventral Tegmental Area/Substantia Nigra Pars Compacta and the Effects of Age. Cereb. Cortex 26, 3413–3427. https://doi.org/10.1093/cercor/bhv172.
Zhong, C., Liu, R., Luo, C., Jiang, S., Dong, L., Peng, R., et al., 2018. Altered structural and functional connectivity of juvenile myoclonic epilepsy: an fMRI study. Neural Plast. 2018, 1–12. https://doi.org/10.1155/2018/7392187.